International Journal
of
Radiology and Diagnostic Imaging

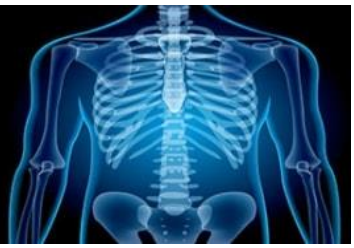

E-ISSN: 2664-4444
P-ISSN: 2664-4436
IJRDI 2019; 2(1): 24-28
Received: 27-12-2018
Accepted: 28-12-2018

Dr. Siddaroodha Sajjan
Assistant Professor,
Department of Radiodiagnosis,
Basaveshwara Medical College,
Chitradurga, Karnataka, India

Dr. Naveen S Maralihalli
Professor and Head,
Department of Radiodiagnosis,
Basaveshwara Medical College,
Chitradurga, Karnataka, India

Correspondence
Dr. Naveen S Maralihalli
Professor and Head,
Department of Radiodiagnosis,
Basaveshwara Medical College,
Chitradurga, Karnataka, India

Radiologic clues to differentiate metastases from other brain pathologies with histopathological correlation

Dr. Siddaroodha Sajjan and Dr. Naveen S Maralihalli

DOI: http://dx.doi.org/10.33545/26644436.2019.v2.i1a.23

Abstract
Introduction: The dissemination of tumour cells to the brain parenchyma does solely occur via the blood stream, as the brain lacks lymphatic vessels. Therefore, tumour cells have to manage survival and adapt to the changed microenvironment within the bloodstream. Several preclinical studies indicate that tumour cells might aggregate with platelets and leucocytes in order to survive.
Methodology: This study was performed at the Department of Radio-diagnosis, and the patients selected for the study were referred from Neurosurgery/Neurology OPD or Emergency department at our hospital, who were clinically suspected to have a space occupying lesion or having history suggestive of metastases. The patients presented with symptoms like headache, motor weakness, diminished vision, double vision, seizure. All patients were seen by appointment, except for the emergency cases. Relevant history of illness and significant clinical findings of all patients were recorded.
Results: Out of 50 cases adenocarcinoma (66%) was the most common histopathology metastasized to the brain followed by squamous cell type (16%), Melanoma (6%), GBM (2%), Oligodendroglioma (2%), liposarcoma (2%) and choriocarcinoma (2%).
Conclusion: In our study most common primary site of metastases was from lung (60%), site of origin of primary was not identified in the 10% cases, third common primary was from breast (6%), kidney (6%), Melanoma(6%) followed by brain (2%), thyroid(2%), Cervix (1%) and uterus(1%).

Keywords: Metastases, brain pathologies, histopathological correlation

Introduction

The propensity of metastatic spread is a hallmark of malignant cancers. A single cancer cell has to overcome several critical obstacles before the successful establishment of a macrometastasis. The “seed and soil” theory postulates that brain metastatic colonization is not only influenced by certain characteristics of the tumour cell (the seed), but also by the microenvironment of the brain parenchyma (the soil). In terms of the “seed”, specific gene expression patterns of brain metastasizing tumour cells were identified that significantly differ from the gene expression patterns of bone metastases in breast cancer model. The “soil”, the brain parenchyma, the pre-existing brain vascular structures as well as astrocytes and microglia influence the establishment of BM. The understanding of the involved molecular mechanism is the prerequisite for the identification of possible `druggable´targets, especially in the prevention of BM [1].

The disconnection of a single tumour cell or a group of tumour cells from extracranial tumour formations (either primary tumour or extracranial metastasis) in a process called epithelial-to-mesenchymal transformation (EMT) is the first mandatory step in the brain metastatic cascade. The process of EMT is characterized by the loss of E-cadherin, an adhesion molecules, as well as the induction of motility [2].

The dissemination of tumour cells to the brain parenchyma does solely occur via the blood stream, as the brain lacks lymphatic vessels. Therefore, tumour cells have to manage survival and adapt to the changed microenvironment within the bloodstream. Several preclinical studies indicate, that tumour cells might aggregate with platelets and leucocytes in order to survive [3].

The passage through the blood brain barrier is the next critical step in the brain metastatic cascade. Here, tumour cells were shown to rest at vascular branching points, presumably due to the reduced shear forces of the blood flow, and use similar mechanisms as leukocytes in

the adhesion cascade to cross the blood brain barrier. The involved adhesion molecules like selectins, integrins, chemokines, heparanases and matrix metalloprotease, represent several theoretically targetable molecules [4].

After the successful passage of the blood brain barrier BM tumour cells have to manage intraparenchymal growth. A real time mouse model of BM using a multi-photon laser-scanning microscope through a chronic cranial window revealed capacious information on the behaviour and properties of BM forming tumour cells after the passage of the blood brain barrier. Tumour cells were shown to stay in close contact with the microvessels directly after the passage through the blood brain barrier and induce either neoangiogenesis or growth via vascular co-option alongside-the pre-existing brain vascular structures. The angiogenic pattern differed depending on the primary tumour subtype. BM from NSCLC were shown to induce early angiogenesis in the outgrowth from micro-to macrometastases, which can be inhibited by antiangiogenic treatment. BM from melanoma presented with growth viavascular co-option and anti-angiogenic treatment did not influence the outgrowth of macrometastases. The growth via vascular co-option is characterized by collective tumour cell migration along pre-existing vessel and relies on integrin signalling. *In vivo* experiments of integrin beta 1 inhibition resulted in prevention of adhesion to the vascular basement membrane und BM outgrowth was attenuated. In line, application of the alpha v integrin inhibitor Intetumumab in a breast cancer BM rat model prevented BM formation and decreased the number of BM. Induction of neo-angiogenesis relies on activation of the vascular endothelial growth factor (VEGF)/hypoxia-inducible factor 1 alpha (HIF 1 alpha) pathway. Hypoxia, induced by fast proliferation an insufficient corresponding neoangiogenesis and can be measured using the HIF 1 alpha index, increases VEGF expression and inconsequence endothelia cell proliferation and blood vessel formation. The resulting vascular formations show pathologic features in their morphology as well as in their growth pattern. Vascular structures as well as vascular density were shown to differ between the primary sites, as melanoma BM were shown to have a lower number of microvessels when compared to carcinomas of the lung or breast. Besides the formation of new blood vessels, the VEGF/HIF 1 alpha axis further influences blood vessel permeability and resulting peritumoural oedema as well as treatment response. Further, high HIF 1 alpha index is associated with resistance to radiotherapy and chemotherapy [5].

So far the time points of detachment from the extracranial tumour lesion, passage of the blood-brainbarrier and outgrowth from micro- to micrometastasis are uncertain. In general, BM are considered a late complication in metastatic cancer. However, screening studies revealed a high incidence of asymptomatic BM. This finding suggests that the detachment of tumour cells and the passage of the blood- brain barrier actually occur early during the disease course but the tumour cells do not grow from the micrometastasis to the macrometastasis status for a certain time. Inline, a real time mouse model of the establishment of BM showed that brain metastatic cells are able to stay dormant in the perivascular niche and persist as asymptomatic micro metastases over prolonged time periods. Therefore molecular characteristic involved in passage of the blood brain barriers and the outgrowth of macrometastases are potentially `druggable´ targets in order to prevent the occurrence of symptomatic BM. Understanding to these key regulators and the time course of brain involvement are precondition to establish clinically applicable BM preventive strategies [6].

Methodology

This study was performed at the Department of Radio-diagnosis, and the patients selected for the study were referred from Neurosurgery/Neurology OPD or Emergency department at our hospital, who were clinically suspected to have a space occupying lesion or having history suggestive of metastases. The patients presented with symptoms like headache, motor weakness, diminished vision, double vision, seizure. All patients were seen by appointment, except for the emergency cases. Relevant history of illness and significant clinical findings of all patients were recorded. Previous investigations were reviewed. Most of the patients were taken for examination without any pre-medication. In uncooperative patients MRI was performed under sedation with supervision of anaesthetist.

Fifty (n = 50) patients, who underwent surgery with histopathological diagnosis were included in the study. Written informed consent was obtained from all the patients for the study. Detailed clinical history was taken in all the patients.

All MR imaging studies were performed with 1.5T superconducting imager (Signa CVi/NVi; GE) using standard head coil. Conventional MR images, FLAIR and DW images were acquired during the same procedure. The T1-weighted spin-echo MR sequence was performed with the following parameters: TR: 500-600 msec, TE: 8-11 msec, FOV: 22-24 cm, matrix size: 320 x 160, section thickness of 5 mm and interslice gap of 1mm. The fast spin-echo T2-weighted sequence was performed with the following parameters: TR: 4000-4500msec, TE: 100 -110 msec, FOV:22-24cm, matrix size: 256 x 256, section thickness of 5 mm and interslice gap of 1mm. Contrast studies were obtained using Magnilek (Gadopentetate Dimeglumine) 0.1 mmol/kg body weight intravenously whenever required. If required, delayed scans were obtained. DW images were acquired in the axial plane by using imaging parameters of 5000/101 to 118 (TR/TE), a slice thickness of 5 mm, an interslice gap of 1.5 mm, a field of view of 20 to 24, a matrix of 128 x 128, bandwidth of 79 kHz, gradient strength of 22 mT, duration of diffusion gradients of 31 ms, and gradient separation of 42 ms, in three orthogonal directions and b values of 1000 sec/mm2. ADC maps were calculated on a pixel-by-pixel basis with software incorporated in the MR imaging unit using following formula ADC = -- [ln (Sb/So)]/b, where Sb is the signal intensity of the ROI obtained through three orthogonally oriented DW images or diffusion trace images, So is the signal intensity of the ROI acquired through reference T2-weighted images, and b is the gradient factor with a value of 1000 sec/mm2.

Image Interpretation: All images are interpreted on synapse picture archiving and communication system (PACS) (Fujifilm) and MRI console monitor (Signa horizon; GE) with adequate gray- scale center level and window width settings. The T1 weighted and T2 weighted signal intensities were compared with gray matter.

Histopathological Examination

The surgical option, resection or biopsy, was chosen by neurosurgeons on the basis of MRI information and tumor location. The tumor components were resected to the greatest extent possible in all patients. The histopathological diagnosis was retrieved from the Department of Pathology.

Results

Table 1: MRI Findings

	MRI Findings	No. of patients (n=50)	%
Multiplicity			
	Multiple	16	32.0
	Single	34	68.0
T1	Heterointense	16	32.0
	Hyperintense	4	8.0
	Hypo intense	20	40.0
	Isointense	10	20.0
T2	Heterointense	21	42.0
	Hyperintense	24	48.0
	Hypointense	1	2.0
	Isointense	4	8.0
FLAIR			
	Heterointense	27	54.0
	Hyperintense	12	16.0
	Hypointense	4	8.0
	Isointense	6	12.0
Blooming on **GRE**		Positive	Negative
		26(52%)	24(48%)
Restriction on **DWI**		Present	Absent
		37(74%)	13(26%)

Out of 50 cases, 34 cases were single metastases and 16 were multiple metastatic lesions Out of 50 cases 20 were hypo intense, 16 were hetero intense, 10 were iso intense and 4 were hyper intense on T1W images. Out of 50 cases 24 were hyper intense, 21 were hetero intense, 4 were iso intense 1 was hypo intense on T2W images. Out of 50 cases 27 were hetero intense, 12 were hyper intense, 6 were iso intense and 4 were hypo intense on T2 FLAIR images. Out of 50 cases 26 showed blooming and 24 not showed blooming on GRE images. Out of 50 cases restriction diffusion was seen in 13 cases and not seen in 37 cases.

Table 2: MRI characteristics with histopathology

MRI characteristics with histopathology	No. of patients (n=50)	%
Type		
Mixed	21	52.0
Solid	12	26.0
Cystic	17	22.0
Cellularity		
High	29	62.0
Low	21	38.0
Necrosis		
Negative	19	38.0
Positive	31	62.0
Bleed		
Negative	29	60.0
Positive	21	40.0
Calcifications		
Present	4	8.0
Absent	46	62.0

Out of 50 cases 21 were mixed solid cystic, 17 were cystic and 12 were cystic. Out of 50 cases 29 cases were high cellular lesions and 21 were with low cellularity. Necrosis was seen 31 cases and necrosis was absent in 19 cases out of 50 cases. Blooming was seen in 21 cases on GRE images out of 50 cases.

Table 3: Pre operative diagnosis on MRI

MRI Diagnosis	No. of patients	%
Metastases	36	72.0
High grade glioma	3	6.0
Low grade glioma	2	4.0
Tuberculoma/Metastases	2	4.0
High Grade Glioma/Metastases	2	4.0
Cerebellar astrocytoma	1	2.0
Hemangioblastoma/Metastases	1	2.0
Meningioma/Metastases	2	4.0
GBM with metastases	1	2.0
Total	50	100.0

Out of 50 cases diagnosis of metastases was given in 36 cases, 3 cases given as high grade glioma turned out to be metastases, 2 cases were given as low grade glioma. Tuberculoma/metastases was given in 2 cases, High Grade Glioma/Metastases was given in 2 cases, Meningioma/Metastases was given 2 cases, cerebellar astrocytoma was given 1 case, 1 case was given as Hemangioblastoma/Metastases and 1 case was given as definite GBM with metastases.

Table 4: Histopathology diagnosis

Histopathology	No. of patients	%
Metastatic adenocarcinoma	33	66.0
Metastatic squamous cell carcinoma	8	16.0
Malignant melanoma	3	6.0
GBM with metastases	1	2.0
Liposarcoma	1	2.0
Vermian anaplastic oligodendroglioma	1	2.0
Choriocarcinoma	1	2.0
Total	50	100.0

Out of 50 cases adenocarcinoma (66%) was the most common histopathology metastasized to the brain followed by squamous cell type (16%), Melanoma (6%), GBM (2%), Oligodendroglioma (2%), liposarcoma (2%) and choriocarcinoma (2%).

Table 5: Primary site of the metastases

Site involved	No. of patients	%
Lung	30	60.0
Unknown primary	5	10.0
Breast	3	6.0
Renal	3	6.0
Brain	2	4.0
Melanoma	3	6.0
Thyroid	2	4.0
Cervix	1	2.0
Uterus	1	2.0
Total	50	100.0

In our study most common primary site of metastases was from lung (60%), site of origin of primary was not identified in the 10% cases, third common primary was from breast (6%), kidney (6%), Melanoma (6%) followed by brain (2%), thyroid (2%), Cervix (1%) and uterus (1%).

Discussion

In our study out of 50 cases 26 showed blooming GRE images suggestive of haemorrhage/calcifications. In a study done by Fink KR *et al.* [7] some metastases, such as melanoma, are T1 hyperintense due to the paramagnetic effects of melanin Hemorrhagic metastases may also demonstrate T1 signal hyperintensity, depending on the age of haemorrhage.

In a study done by Lassman AB *et al.* [8] hemorrhage into metastases may produce sudden severe headache, coma, or stroke-like focal neurologic findings; however, in an older clinicopathologic series of 15 patients with hemorrhagic metastases, the presentation was acute in only three (20%), whereas the onset was gradual in five (33%) and subacute in the remainder (approximately 50%) Tumors particularly prone to hemorrhage include melanoma, renal cell and thyroid carcinomas, and choriocarcinoma. Lung cancer is not a typically hemorrhagic tumor; however, the high frequency of brain metastases from pulmonary primaries makes lung the most frequent hemorrhagic metastasis.

Out of 50 cases restriction diffusion (Low ADC) was seen in 13 cases and not seen in 37 cases.

In a study done by Krabbe K *et al.* [9] ADC in contrast-enhancing tumour were significantly higher in cerebral metastases than in high-grade gliomas (P<0.05). ADC in oedema around cerebral metastases was significantly higher than those around high-grade gliomas (P<0.02).

In a study done by Fink KR *et al.* [7] DWI usually demonstrates facilitated diffusion (i.e., bright on apparent diffusion coefficient (ADC) map), rather than diffusion restriction. In our study out of 50 cases, heterogeneous enhancement was seen in 24 cases, 23 cases showed ring enhancement and homogeneous enhancement was seen in 3 cases on T1W post contrast images. In a study done by Moiyadi A *et al.* [10] the classical appearance of a metastasis is a solid enhancing mass with well-defined margins and extensive edema. Occasionally, central necrosis produces a ring enhancing mass. In a study done by Prabhash K *et al.* [11] in metastases solid, nodular or irregular ring patterns of enhancement are seen.

Out of 50 cases 16 cases showed increased lipid lactate peak, in 9 cases increased choline and lipid lactate peak, 9 cases showed increased choline peak and in 16 cases MRS was non-contributory. In a study done by Mills SJ *et al.* [12] MRS in comparing lipid and macromolecule signals in cerebral metastases (n¼34) and GBM (n¼25) and reported significantly higher values in metastases.

In a study done by Chernov *et al.* [13] reported increased mobile lipid content and elevated Lip/nCr in cerebral metastases arising from a colorectal primary when compared with metastases from histologically distinct primary tumours. In a study done by Prabhash K *et al* [11]suppressed NAA and Creatinine. Elevated choline and lactate levels are seen in metastases. Disproportionate prelesional edema was seen in 42 cases as compared to that of the size of the lesion in our study.

In a study done by Mills SJ *et al.* [12] the degree of peritumoural oedema varies from virtually none to (more commonly) extensive surrounding oedema in metastases. A greater degree of perilesional signal change, commonly referred to as oedema although the underlying content in glioma is more complex, is reportedly indicative of metastatic disease rather than glioma. A more recent MRI study of 26 metastases and 22 high-grade gliomas (HGG) evaluated the peri- tumoural oedema to tumour area ratio, and found significant differences between HGG (0.69+/=0.41) and metastases (2.41=/+1.63), P<0.001.

In a study done by Prabhash K *et al.* [11] the classical appearance of a metastasis is a solid enhancing mass with well‐defined margins and extensive edema.

In a study done by Chi A *et al.* [14] Brain metastases are usually found at the junction of the grey and white matters, with circumscribed margins and large amounts of vasogenic edema relative to the size of the lesion.

In our 50 cases diagnosis of metastases was given in 36 cases, 3 cases given as high grade glioma, 2 cases were given as low grade glioma, Tuberculoma/metastases was given in 2 cases, High Grade Glioma/Metastases was given in 2 cases, Meningioma/Metastases was given 2 cases, cerebellar astrocytoma was given 1 case, 1 case was given as hemangioblastoma/Metastases and 1 case was given as definite GBM with metastases.

In a study done by Mills SJ *et al.* [12] shows metastatic disease differentiation from multifocal glio- blastoma multiforme (GBM) and tumour mimics such as infection or tumefactive demyelination can be difficult.

In a study done by Prabhash K *et al.* [11] shows cystic lesions in the brain in an immunocompetent individual include brain metastases, brain abscess, tuberculoma, neurocysticercosis, primary tumor of brain, and sarcoidosis. Differentiating these cysts on the basis of imaging findings alone is difficult. In a study done by Lassman AB *et al* [8] most contrast-enhancing lesions in a cancer patient are metastases, but the common differential diagnosis includes primary brain tumor, abscess, infarction, radiation necrosis (in a previously treated patient), granuloma, and demyelination In our study adenocarcinoma (66%) was the most common histopathology metastasized to the brain followed by squamous cell type (16%).

In a study done by Nguyen LN *et al.* [15] the over whelming majority, 31 patients (79%), had adenocarcinoma; 2 patients had small cell carcinoma and one had squamous cell carcinoma.

Conclusion

- Majority of metastases were intra axial and supratentorial compartment
- Most common primary metastases to the brain is from lung
- MRI helps in accurate localization metastases.
- MRI is the modality of choice in analysing tissue characteristics of the metastases
- In adult presenting with ring enhancing lesion metastases needs to considered in the differentials.
- MRS and DWI Imaging helps in narrow down the differentials.
- MRI is the preoperative study of choice to narrow the differential diagnosis and help surgical resection.

References

1. Hendrick RE. The AAPM/RSNA physics tutorial for residents. Basic physics of MR imaging: an introduction. Radiographics: a review publication of the Radiological Society of North America, Inc, quiz 47-8. PubMed PMID: 7938771. 1994; 14(4):829-46
2. Hendee WR. Cross sectional medical imaging: a history. Radiographics: A review publication of the Radiological Society of North America, Inc. 1989;

9(6):1155-80.
3. Pillai JJ KL. Brain Magnetic Resonance Spectroscopy. 4 ed. John R. Haaga CFL, Robert C. Gilkeson, editor. St. Louis. Mosby. 2003, 30.
4. Nomura Y, Sakuma H, Takeda K, Tagami T, Okuda Y, Nakagawa T. Diffusional anisotropy of the human brain assessed with diffusion-weighted MR: relation with normal brain development and aging. AJNR American journal of neuroradiology. 1994; 15(2):231-8.
5. Schaefer PW, Grant PE, Gonzalez RG. Diffusion-weighted MR imaging of the brain. Radiology. 2000; 217(2):331-45.
6. Joseph P. Cousins. Clinical MR Spectroscopy: Fundamentals, Current Applications, and Future Potential. AJR. 1995; 164:1337-1347.
7. Fink KR, Fink JR. Imaging of brain metastases. Surgical neurology international. 2013; 4(Suppl 4):S209.
8. Lassman AB, DeAngelis LM. Brain metastases. Neurologic clinics. 2003; 21(1):1-23.
9. Krabbe K, Gideon P, Wagn P, Hansen U, Thomsen C, Madsen F. MR diffusion imaging of human intracranial tumours. Neuroradiology. 1997; 39(7):483-9.
10. Moiyadi A, Pantvaidya G, Arya S, Shetty P. Cystic metastasis versus brain abscess: Role of MR imaging in accurate diagnosis and implications on treatment. Journal of Cancer Research and Therapeutics. 2010; 6(3):356.
11. Prabhash K, Noronha V, Tandon N, Joshi A, Sharma V. A systematic approach to diagnosis of cystic brain lesions. South Asian Journal of Cancer. 2013; 2(2):98.
12. Mills SJ, Thompson G, Jackson A. Advanced magnetic resonance imaging biomarkers of cerebral metastases. Cancer Imaging. 2012; 12(1):245-52.
13. Chernov MF, Ono Y, Kubo O, Hori T. Comparison of 1H-MRS- detected metabolic characteristics in single metastatic brain tumors of different origin. Brain Tumor Pathol. 2006; 23:3540.
14. Chi A, Komaki R. Treatment of Brain Metastasis from Lung Cancer. Cancers. 2010; 2(4):2100-37.
15. Nguyen T, DeAngelis LM. Treatment of brain metastases. J Support Oncol. 2004; 2(5):405-10.